Optimization Design of Powertrain Parameters for Electromechanical Flywheel Hybrid Electric Vehicle

Binbin Sun, Tianqi Gu, Pengwei Wang, Tiezhu Zhang and Shubin Wei

Abstract—**In order to improve the energy utilization efficiency and driving range of electric vehicle, an electromechanical flywheel hybrid system based on planetary gear power split is proposed in this study. First, based on the working principle of planetary gear, the performance of the system under six topologies was analyzed. The optimal design schemehe was confirmed. Specially, the speed regulating motor and the flywheel connect with sun gear and ring gear respectively, the power output from carrier. Then, to meet the design requirement of the vehicle, the parameters of electromechanical flywheel hybrid device, the drive motor and the transmission were optimized. Finally, a vehicle dynamic simulation model was constructed to analyze the dynamic and economic performances of the vehicle under different conditions. Results show that, compared with the original vehicle driven by a single motor, the new hybrid system designed is able to improve the vehicle economy effectively while maintaining the power performance. Under J1015, NEDC and HWFET cycles, the average operating efficiencies of the power system are increased by 8.2%, 5.6% and 4.3%.**

Index Terms—**electromechanical flywheel, planetary gear, optimization design, vehicle dynamic model, cycle efficiency**

I. Introduction

ENERGY crisis and environmental pollution are the two major problems inhibiting current social development. As one of the main contributors to the current petroleum energy consumption and pollution emissions, traditional oil-fueled vehicle still accounts for the increasing negative effect[1-2]. Pure electric vehicle is considered as an effective scheme to solve the current energy and environmental problems, owe to the advantages in higher comfort, low noise, higher cleanness, zero pollution and higher energy efficiency [3-4]. However, the insufficient driving range is still a common problem existing in various form of electric vehicle, which is also a key factor limiting its rapid development [5].

Flywheel energy storage technology, which has the advantages of high energy conversion efficiency and high power density, attracts extensive attention from the automotive industry [6-8]. From the perspective of energy input and output methods, the current common flywheel energy storage systems can be summarized into two types. One is the electrical energy storage system, and the other one is the mechanical energy storage system [9]. Due to the limited energy storage capacity, high energy storage and low self-consumption, achieved through the of ultra-high-speed and high-efficiency design, are essential to the electric and mechanical flywheel systems. To meet the special design requirements, composite material flywheel, magnetic bearing and vacuum chamber have to be used [10]. The technical difficulty and high-cost limit the application of the two kind flywheels in vehicle.

Owing to the characteristics of vehicle driving conditions, especially the frequent and intermittent braking operation under urban conditions [11-12], the energy supplement of flywheel storage system by vehicle brake is intermittent but continuous. This special feature is conducive to the lower design requirements of flywheel energy storage, especially the self-consumption rate.

Based on the above analysis, a unique flywheel hybrid device using planetary gear with non-ultra-high speed is proposed and designed. First of all, structure scheme of a electric vehicle driven by electromechanical flywheel hybrid device is introduced. In the second part, topological structure of the flywheel hybrid device is analyzed and the optimal scheme is determined. Then, parameters of the vehicle hybrid system are designed and optimized in the third part. Furthermore, in the fourth part of the paper, dynamic model of the electromechanical flywheel hybrid electric vehicle is established. Finally, the vehicle performance analysis and verification are carried out.

II. Structure Scheme of Electromechanical Flywheel Hybrid Electric Vehicle

Fig. 1 shows the electric vehicle driven by the electromechanical flywheel hybrid system. On the basis of the prototype vehicle driven by a single front motor, the new vehicle is equipped with the electromechanical flywheel

Manuscript received October 15, 2021; revised March 3, 2022. This work was supported in part by the National Natural Science Foundation Project of China under Grant 51805301 and 52102465, the Natural Science Foundation Project of Shandong under Grant ZR2019BEE043, the Postdoctoral Science Foundation of China and Shandong under Grant 2020M680091 and 202003042, the Major Innovation Projects in Shandong under Grant 2020CXGC010405 and 2020CXGC010406.

Binbin Sun is a Professor of School of Transportation and Vehicle Engineering, Shandong University of Technology, Zibo, 255000 PR China. (e-mail: sunbin_sdut@126.com).

Tianqi Gu is a graduate student of School of Transportation and Vehicle Engineering, Shandong University of Technology, Zibo, 255000 PR China. (e-mail: tianqi.gu@outlook.com).

Pengwei Wang is a Professor of School of Transportation and Vehicle Engineering, Shandong University of Technology, Zibo, 255000 PR China. (corresponding author to provide phone: 86-13287825788; e-mail: wpwk16@163.com).

Tiezhu Zhang is a Professor of School of Transportation and Vehicle Engineering, Shandong University of Technology, Zibo, 255000 PR China. (e-mail: qdzhangtz@163.com).

Shubin Wei is a graduate student of School of Transportation and Vehicle Engineering, Shandong University of Technology, Zibo, 255000 PR China. (e-mail: 305027630@qq.com).

hybrid device in the rear drive shaft. The vehicle controller (VCU) is responsible for the control of the vehicle power system by collecting information such as vehicle speed, accelerator or brake pedal opening and status parameters of energy power system.

Compared with the original scheme, with the help of the rear electromechanical flywheel, a smaller front drive motor is used in the new hybrid electric vehicle. The deign is conducive to improve the working efficiency of the front motor when it operates under low-load conditions. In addition, the electromechanical flywheel hybrid device is able to intervene into the driving or braking process of the vehicle in real time according to the working condition, consequently, further optimization of vehicle energy utilization efficiency can be achieved. Tab. 1 shows the basic performance parameters of the new hybrid vehicle.

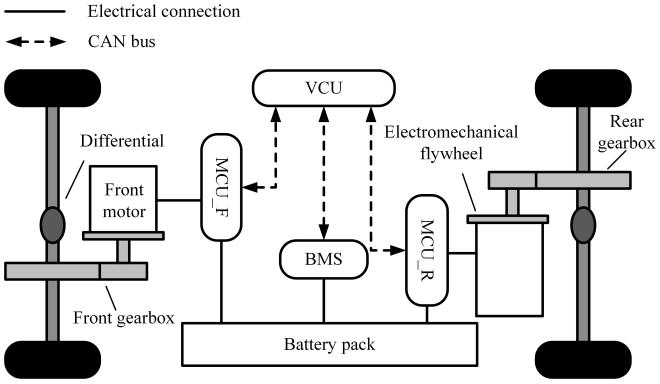

Fig. 1 Electromechanical flywheel electric vehicle

Tab. 1 Basic performance parameters of the hybrid vehicle

Basic parameters		Power performance indicators	
Curb weight/kg	1932	Maximum design speed/km·h^{-1}	150
Loading mass/kg	450	Maximum design gradeability /%	22
Frontal area /m^2	2.47	Acceleration time form 0 to 100 km·h$^-$ /s	12

III. Topological Structure Design of Electromechanical Flywheel Hybrid Device

In the electromechanical flywheel device, a single-row planetary gear mechanism is designed to achieve speed coupling. The sun gear, ring gear and planet carrier have the following speed relationship.

$$n_c = \frac{1}{1+k} n_s + \frac{k}{1+k} n_r \tag{1}$$

Where, n_s, n_r, n_c are the rotate speed of the sun gear, ring gear and planet carrier, respectively. k is the characteristic parameter of the planet row. It is the ratio between the number of teeth in the ring gear and that of the sun gear.

As the energy loss in stable operation is negligible, the sun gear, ring gear and planet carrier present the torque constraint as follow.

$$T_c = -(1+k)T_s = -[(1+k)/k]T_r \tag{2}$$

Where, T_s, T_r, T_c are the rotational speeds of the sun gear, ring gear and planet carrier, respectively.

According to the relations between the adjustable-speed motor, flywheel, output shaft and planetary gear, six structural schemes is obtained, as shown in Tab. 2.

Tab. 2 Connection relationships of electromechanical flywheel device

Mechanical connection scheme	Adjustable-speed motor	Flywheel	Output shaft
1	Sun gear	Ring gear	Planet carrier
2	Sun gear	Planet carrier	Ring gear
3	Planet carrier	Sun gear	Ring gear
4	Planet carrier	Ring gear	Sun gear
5	Ring gear	Sun gear	Planet carrier
6	Ring gear	Planet carrier	Sun gear

As the flywheel is unable to operate independently, the adjustable-speed motor is designed to adjust and control the operative mode of the flywheel. Consequently, the output torque of the flywheel depends on the torque of the adjustable-speed motor. As the the characteristic parameter of the planet row is greater than 1, according to the torque constraint formula, the output torque of scheme 1 in Tab. 2 is the highest. In addition, owing to the largest torque amplification factor of the adjustable-speed motor in scheme 1, smaller torque is required by the adjustable-speed motor when the output torque is constant. This advantage is conducive to integration and miniaturization design of the adjustable-speed motor. Given the comprehensive analysis, scheme 1 is selected as the topology scheme of the electromechanical flywheel device.

IV. Parameter Design of Vehicle Power System

A. Parameter design of the front motor

According to the vehicle performance parameters in Tab. 1, J1015, NEDC and HWFET cycles, represent urban, urban and suburban, and high-speed working conditions, are selected as reference working conditions to calculate the high-frequency operating characteristics of the vehicle. As shown in Tab. 3, based on mathematical statistics, the high frequency ranges of speed-power and speed-torque are obtained. According to the statistical data, in terms of vehicle speed and power, J1015 high-frequency working condition is characterized by low speed and low power. Low speed and low power as well as medium speed and medium power are frequent in NEDC working condition. Under HWFET cycle, the vehicle operate under condition of high speed and high power frequently.

Tab. 3 Distribution law of working condition characteristics

High frequency range	Working condition		
	J1015	NEDC	HWFET
Vehicle speed-power	(0-40km·h^{-1}, 0-25kW)	(0-40km·h^{-1}, 0-25kW) (40-70km·h^{-1}, 25-50kW)	(70-90km·h^{-1}, >75kW)
Vehicle speed-torque	(0-40km·h^{-1}, 0-250N·m) (0-40km·h^{-1}, >1000N·m)	(0-40km·h^{-1}, 0-250N·m) (40-70km·h^{-1}, 0-250N·m)	(>70km·h^{-1}, 0-500N·m)

Moreover, in terms of speed-torque, J1015 high-frequency working condition is characterized by low speed and low-load as well as low speed and high load. NEDC presents the frequent characteristic of low speed and low load as well as medium speed and low load. Under HWFET cycle, the vehicle operate under condition of high speed and medium load frequently.

According to the speed-power and speed-torque distribution characteristics of the hybrid vehicle, to achieve efficient operation, the parameter design of the front motor should meet the follows.

First of all, to meet the power requirements of the front motor under high frequency, medium and low load conditions, the rated power is designed between 45kW and 50 kW.

Secondly, to improve the front motor efficiency, the rated speed of it should cover the vehicle speed, from 50km·h^{-1} to 60km·h^{-1}. This design is helpful for matching the urban high-frequency operation of the vehicle. Furthermore, in order to meet the requirements of the vehicle highest design speed, the peak speed of the front motor is set to 13000r·min^{-1}.

Then, the rated torque output by the front motor to the wheel should be greater than 700N·m so as to reduce the overload operation frequency under urban high-frequency conditions. The design is able to increase the proportion of normal operation, and improve the motor working efficiency consequently.

Finally, considering the design margin, the parameters of the front motor are confirmed as shown in Tab. 4.

Tab. 4 Parameters of front motor

Motor type	Permanent magnet synchronous motor
Rated speed/(r·min^{-1})	4000
Rated power/kW	45
Rated torque/N·m	144
Peak speed/(r·min^{-1})	13000
Peak power/kW	70
Peak torque/N·m	227

B. Parameter optimization design of flywheel

The state of energy, SOE, is used to indicate the energy storage capacity of flywheel. For flywheel energy storage device, the key factor that affects the flywheel size is the energy capacity E_{cap}, which is mainly determined by two factors, specially, energy release acceleration and energy storage deceleration.

$$E_{cap} = \frac{1}{2} J \left(n_{max}^2 - n_{min}^2 \right) \tag{3}$$

Where, J is the moment of inertia of the flywheel, n_{max}^2 is the highest rotate speed of flywheel, n_{min}^2 means the lowest operating speed. Furthermore, J is the function of flywheel mass and radius.

$$J=mr^2 \tag{4}$$

Where, m is the flywheel mass, r is the flywheel radius.

The peak energies required by the electromechanical flywheel hybrid electric vehicle under J1015, NEDC and HWFET are calculated as shown in Tab. 5. The positive peak energy means the driving energy required by the vehicle. The negative number indicates the braking energy that can be recovered by the vehicle.

Tab. 5 Released and recovered peak energy of the hybrid vehicle

Working condition	Required peak energy /kW·h	Recyclable peak energy/kW·h
J1015	+0.2179	-0.01008
NEDC	+1.0383	-0.0062
HWFET	+0.4831	-0.0124

Based on the energy data, the maximum and second driving energy required by the vehicle under the three working conditions is 1.0383kW·h and 0.4831kW·h, which far exceed the peak recovery energy. Obviously, the driving energy required by the vehicle should be achieved by both the front motor and the electromechanical flywheel system. Given the above analysis, the energy storage conditions of flywheels with different proportions are calculated, as shown in Tab. 6.

Based on comprehensive analysis, the flywheel design storage energy is designed as 0.25kW·h. First of all, the energy storage value is able to cover the recoverable peak energy and most of the required driving energy range. Furthermore, the size of the designed flywheel can meet the limited space design requirements of the vehicle. According to the dynamic formulas of the flywheel, the parameters are confirmed as shown in Tab. 7.

Tab. 6 Different proportions of energy stored in the flywheel

Flywheel energy/kW·h	Proportion/ %	Moment of inertia/kgm^2	Radius/m	Volume/ 10^{-3}m^3
0.4831	100	1.058	0.1712	9.208
0.4348	90	0.9519	0.1667	8.73
0.3865	80	0.8462	0.1619	8.235
0.3382	70	0.7404	0.1565	7.694
0.2899	60	0.6347	0.1506	7.125
0.2416	50	0.5289	0.1439	6.505
0.1932	40	0.4229	0.1361	5.819
0.1449	30	0.3172	0.1266	5.035
0.0966	20	0.2115	0.1144	4.112
0.0483	10	0.1057	0.0962	2.909

Tab. 7 Parameters of the flywheel

Flywheel energy storage/kW·h	0.25
Moment of inertia	0.5473
Radius/m	0.1451
Column height/m	0.1
Volume/m^3	0.01451
Mass/kg	113.9

C. Parameter design of adjustable-speed motor

When the vehicle operates under high speed, higher than 90% of the maximum design speed, there may be insufficient flywheel energy for operation. Under this operation, the front motor and the adjustable-speed motor should provide all the driving power required by the vehicle. Consequently, the

rated power required by the electromechanical flywheel electric vehicle is equal to the sum of the rated power of the two motors. The rated power provided by the front motor and adjustable-speed motor should be higher than that in the original vehicle.

$$\begin{cases} P_{\text{f\_e}} + P_{\text{srm\_e}} = P_{\text{e}} \\ P_{\text{e}} \approx \dfrac{0.9v_{\max}}{3600\eta_{\text{T}}}\left(mgf + \dfrac{C_{\text{D}}A(0.9v_{\max})^2}{21.15}\right) \end{cases} \tag{5}$$

Where, $P_{\text{f\_e}}$ is the rated power of the front motor, $P_{\text{srm\_e}}$ is the rated power of the adjustable-speed motor, P_{e} is the rated power required by the electric vehicle, C_{D} is the drag coefficient of the electric vehicle, A is the windward sectional area, $v_{\max}$ is the maximum design speed of the electric vehicle, η_{T} is the transmission efficiency.

According to the maximum gradeability of the vehicle, the peak power of the adjustable-speed motor can be confirmed as follow.

$$P_{\max} = \frac{v}{3600\eta_{\text{T}}}\left(mgf\cos\alpha_{\_\max} + mg\sin\alpha_{\_\max} + \frac{C_{\text{D}}Av^2}{21.15}\right) \tag{6}$$

Where, $P_{\max}$ is the peak power of the adjustable-speed motor; $\alpha_{\max}$ is the maximum gradeability.

Given the above analysis, the parameter of the adjustable-speed motor should meet the follows.

First of all, to improve the matching degree between the high-efficiency working area of the adjustable-speed motor and the high-speed working condition, the rated speed of the adjustable-speed motor should cover the vehicle speed from 50km·h^{-1} to 60km·h^{-1}, the peak speed of the motor should meet the vehicle high speed range between 140km·h^{-1} and 150km·h^{-1}.

Secondly, the rated torque output by the adjustable-speed motor to rear wheels should be greater than 300N·m so as to compensate for the torque difference required by the front motor.

Finally, considering the design margin, the parameters of the adjustable-speed motor are confirmed as shown in Tab. 8.

Tab. 8 Parameters of the adjustable-speed motor

Motor type	Permanent magnet synchronous motor
Rated speed /r·min^{-1}	4000
Rated power /kW	25
Rated torque /N·m	35
Peak speed/ r·min^{-1}	13000
Peak power /kW	40
Peak torque /N·m	60

D. Parameter optimization design of transmission

According to the maximum design gradeability and the maximum design speed of the vehicle, based on the following kinematic relationship, the range of the front transmission ratio is determined within the range from 7.3 to 8.8. Under J1015 cycle, if the front transmission ratio is designed as 8.5, higher efficiency of the front motor is obtained as shown Tab. 9. Specially, compared to the 7.5 transmission ratio, the cycle efficiency of the front motor increases 1.14%. By the use of 8.5 transmission ratio, some operations under low-speed and low-efficiency working condition area are optimize to the medium-speed and high-efficiency working condition, which is helpful for the improvement of the motor efficiency.

$$\begin{cases} i \geq \dfrac{\left(mgf\cos\alpha_{\_\max} + mg\sin\alpha_{\_\max} + \dfrac{C_{\text{D}}Av^2}{21.15}\right)r}{T_{\max}\eta_{\text{T}}} \\ i \leq \dfrac{0.377rn_{\max}}{v_{\max}} \end{cases} \tag{7}$$

Where, i is the front transmission ratio, r is the vehicle wheel radius.

Tab. 9 Relationship between transmission ratio and motor efficiency

Transmission ratio	Average efficiency of the motor under J1015/%	
	Efficiency/%	Efficiency increase/%
i=7.5	84.99	0
i=8	85.47	0.56
i=8.5	85.96	1.14

The power output route of the rear axle follows the order as: from motor/flywheel to planetary gear mechanism, then to rear axle reducer, finally to wheel. As the power transmission route involves multiple components, multi-objective genetic algorithm is used to optimize the characteristic parameter k of the planetary and the rear axle transmission ratio i_2. In order to minimize the energy consumption of genetic individuals and the included angle of normal vectors between a and b simultaneously, the fitness evaluation function of the multi-objective genetic algorithm is designed as follow.

$$\min\begin{cases} f_1(x_1,x_2,x_3) = J(k,i,n_{\text{fw}}) \\ f_2(x_1,x_2) = \theta(k,i) \end{cases} \tag{8}$$

$$\text{st}\begin{cases} 0 < k \leq 100 \\ 0 < i_2 \leq 10 \\ 10000 < n_{\text{fw}} \leq 20000 \end{cases} \tag{9}$$

Where, n_{fw} is the rotational speed of the flywheel; $\theta(k,i)$ is the angle of normal vectors between a and b.

Tab. 10 shows the final optimization result of k and i under under different flywheel SOEs. Within the effective value range, considering the design allowance, the characteristic parameter k of the planetary gear is set as 2.2. The transmission ratio of the rear axle reducer is designed as 6.2.

Tab. 10 Optimization results of different flywheel SOE

Flywheel SOE	Transmission ratio	k	Energy consumption/kJ	Minimum θ/rad
0.5	3.9	4.7	4.72	0.2871
0.6	4.7	3.3	4.70	0.2793
0.7	5.6	2.6	4.69	0.2757
0.8	6.2	2.2	4.66	0.2588
0.9	7.1	1.9	4.63	0.2543
1.0	7.8	1.8	4.61	0.2425

V. VEHICLE DYNAMIC MODELING

A. Construction of vehicle performance simulation platform

As shown in Fig. 2, based on the MATLAB/SIMULINK

platform, an electromechanical flywheel electric vehicle simulation platform is built. The platform mainly consists of driver module, powertrain system, communication system, control system and some other sub-modules. The driver module uses PID algorithm to calculate the driving/braking torque required by the vehicle. The powertrain system is responsible for the status update and data feedback of the vehicle, battery, front motor, and electromechanical flywheel hybrid device. The communication system is designed to achieve the transmission of vehicle control and status data. The control system is used to conduct the control of the vehicle working mode and energy management.

B. Sub-module of powertrain system

Taking the electromechanical flywheel hybrid power system as an example. The powertrain model is established as shown in Fig. 3. It consists of sub-models such as battery module, motor module, electromechanical flywheel system module and vehicle dynamic module. The powertrain system model is mainly responsible for generating and transmitting power, to realize the state update and control of the entire vehicle and its components according to the control signal.

(1) Flywheel model

As the energy and power source, the flywheel is designed to output store energy or power according to the vehicle status. As shown in Fig. 4, the flywheel model is responsible for calculating the speed, torque, SOE and power. According to the connection relationship between the flywheel and the ring gear, the speed and torque of the flywheel are calculated as follows.

$$n_{\mathrm{fw}} = n_{\mathrm{r}} i_{\mathrm{fw\text{-}r}} \tag{10}$$

$$T_{\mathrm{fw}} = \frac{T_{\mathrm{r}}}{i_{\mathrm{fw\text{-}r}}} \tag{11}$$

Where, $n_{\mathrm{fw}}$is the flywheel speed, $n_{\mathrm{r}}$is the speed of the ring gear, T_{fw} is the flywheel torque, T_{r} is the ring gear torque, $i_{\mathrm{fw-r}}$ is the transmission ratio from the flywheel to the ring gear.

The SOE is directly related to the flywheel speed, and is calculated by the following formula.

$$SOE = \frac{n_{\mathrm{fw}}}{n_{\mathrm{fw\_max}}} \times 100\% \tag{12}$$

Where, n_{fw} is the actual speed of the flywheel, $n_{\mathrm{fw\_max}}$ is the maximum operating speed of the flywheel.

When the flywheel recovers or releases energy, the power is derived as follow.

$$P_{\mathrm{fw}} = T_{\mathrm{fw}} n_{\mathrm{fw}} K \tag{13}$$

Where, P_{fw} is the flywheel power, a positive value of P_{fw} indicates the released energy. while, a negative value of P_{fw} indicates the absorbed energy. T_{fw} is the flywheel torque, K is the unit conversion factor.

(2) Planetary gear model

The planetary gear model is designed for calculating the speed and torque of the sun gear, ring gear and planet carrier. Based on the speed coupling relationship, the speed equation of the device is confirmed.

$$n_{\mathrm{c}} = \frac{1}{1+k} n_{\mathrm{s}} + \frac{k}{1+k} n_{\mathrm{r}} \tag{14}$$

Where, n_{s}, n_r, n_c are the rotate speeds of the sun gear, ring gear and planet carrier, respectively.

As the energy loss of the planetary gear under stable operation is negligible, the torque relationship of the sun gear, ring gear and planet carrier is derived as follow.

$$T_{\mathrm{c}} = -(1+k) T_{\mathrm{s}} = -[(1+k)/k] T_{\mathrm{r}} \tag{15}$$

Where, T_{s}, T_{r}, T_{c} are the rotate speed of the sun gear, ring gear and planet carrier, respectively.

VI. Vehicle Performance Analysis

(1) Dynamic analysis

As the output torque shown in Fig. 5, both the original scheme (the vehicle driven by single front motor) and the proposed scheme (the vehicle driven by hybrid power system) are able to meet the requirements of maximum design gradeability (22%). The hybrid power system presents better dynamic property as it can provide greater backup torque, which means the designed power-train system using the hybrid scheme improves the climbing performance.

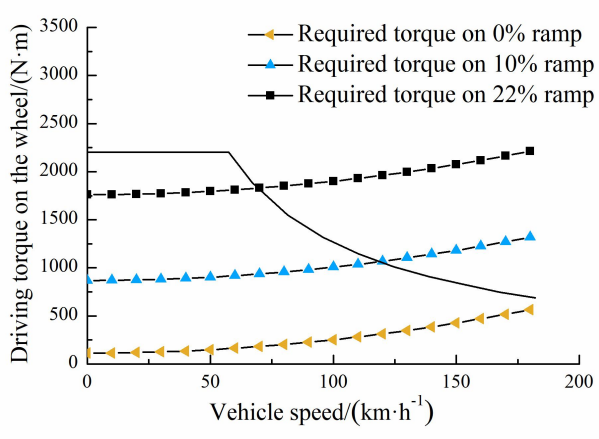

(a) The original scheme

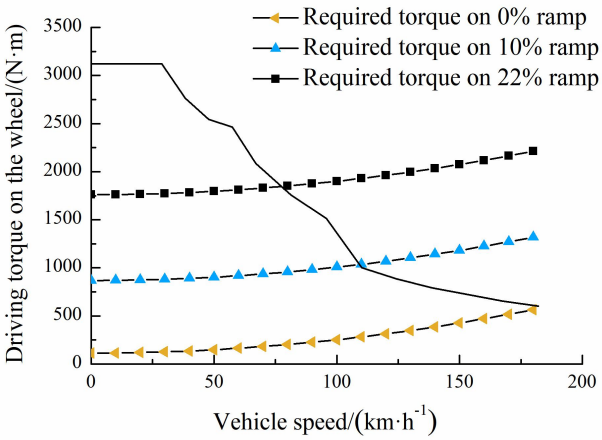

(b) The new scheme

Fig. 5 Comparison of climbing performance

Moreover, as shown in Fig. 6, under J1015, NEDC and HWFET working conditions, regardless of low speed or high speed operations, the two schemes meet the acceleration power requirement. However, compared with the vehicle driven single front motor, the four wheel drive vehicle with electromechanical flywheel hybrid system has higher peak power and better acceleration performance.

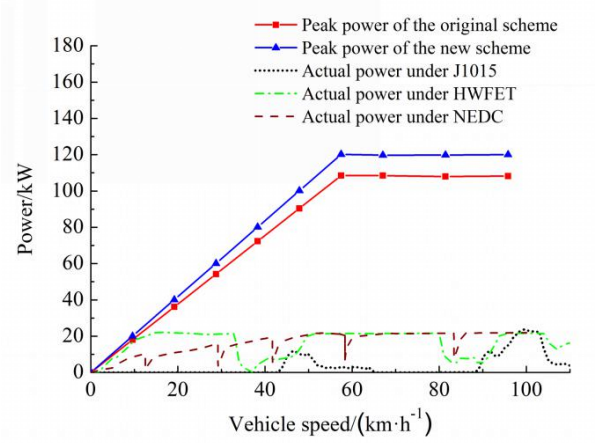

Fig. 6 Comparison of acceleration performance

(2) Economic analysis

As shown in Fig. 7 (a), under J1015 working condition, limited by the dynamic topology scheme, low-efficiency operation the motor is ineluctable within the original vehicle driven by the single front motor domain A1 and A2, where motor works under low-medium speed and high load conditions. It leads to the low efficiency of the vehicle.

As shown in Fig. 7 (b), owing to the electromechanical flywheel hybrid system, the operation efficiency of the front motor improves significantly. Specially, compare with the original scheme, the operating points of the front motor are optimized from the low-efficiency domain A1 and A2 to the high-efficiency domain B1 and B2. Consequently, the efficiency of the new vehicle is improved.

As shown in Fig. 8, under J1015 and NEDC working conditions, compared with the original scheme, owing to the advantage of multi power drive, the electromechanical flywheel hybrid power-train system increase the average efficiency of the front motor by 8.3% and 5.6%, respectively. The main reason is that, in comparation with the original vehicle, ensuring the premise of vehicle dynamics, the front motor of the electromechanical flywheel hybrid electric vehicle adopts a miniaturized design. This special design is helpful for the improvement of the motor efficiency when it operates alone under the high-frequency and low-load conditions. Under NEDC cycle, as the proportion of urban low-load conditions decreases, the efficiency improvement of the front motor decreases.

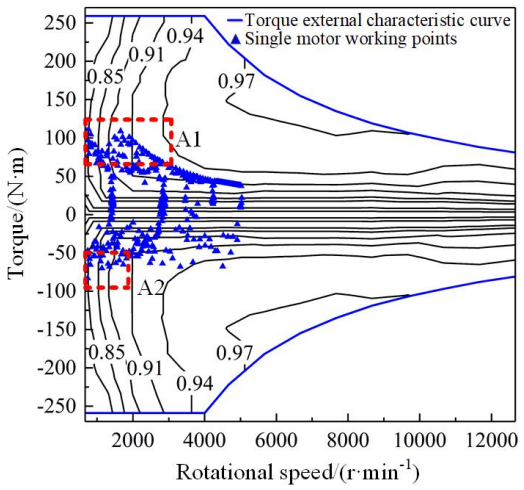

(a) Motor efficiency distribution of the original scheme

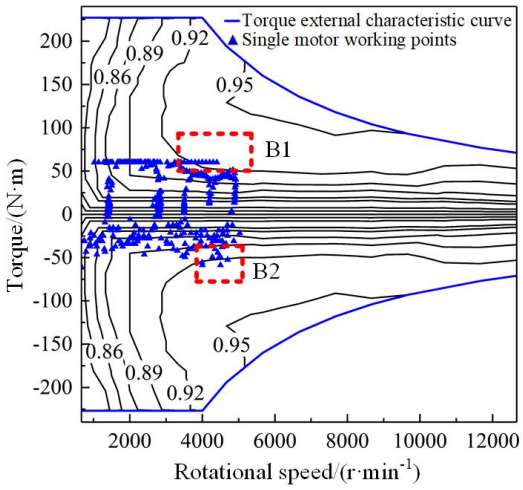

(b) Motor efficiency distribution of the proposed scheme

Fig. 7 Motor efficiency under J1015 cycle

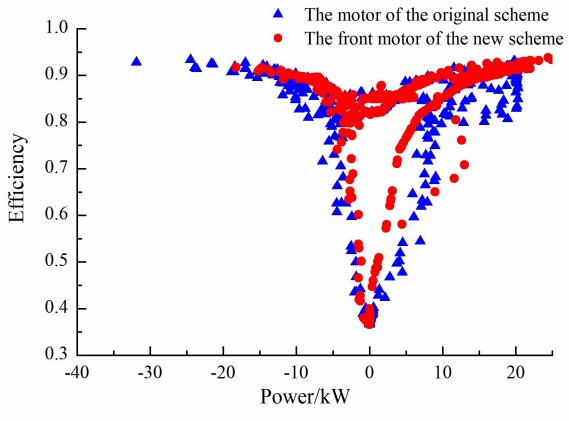

(a) Motor efficiency under J1015

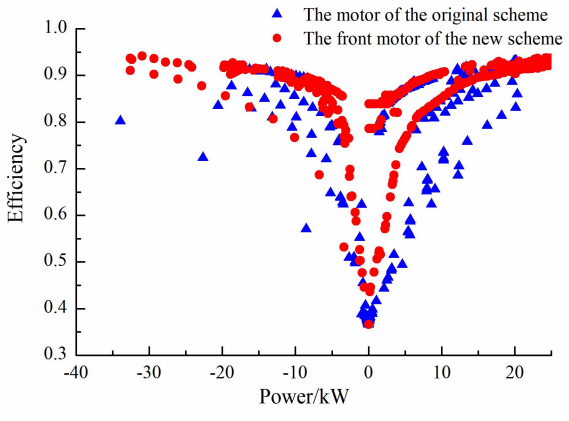

(b) Motor efficiency under NEDC

Fig. 8 Comparison of motor efficiency

As shown in Tab. 11, under J1015, NEDC and HWFET working conditions, compared with the original scheme driven by single front motor, the proportion of the electromechanical flywheel hybrid power-train under high-efficiency operations (system efficiency >90%) increases by 19.9%, 6.1% and 9.2% respectively. More importantly, the proportion of that under low efficiency conditions (system efficiency <80%) decreases by 13%, 2.4% and 0.7% respectively. Consequently, the average efficiency increases by 8.2%, 5.6% and 4.3%, respectively.

Tab. 11 Efficiency of the power-train system

Working condition	Scheme	Efficiency interval			
		>90%	85-90%	80-85%	<80%
J1015	Hybrid power	41.6%	23.2%	24.1%	11.1%
	Single motor	21.7%	31.4%	22.8%	24.1%
NEDC	Hybrid power	23.5%	31.6%	8.6%	36.3%
	Single motor	17.4%	36.1%	7.8%	38.7%
HWFET	Hybrid power	89.2%	7.3%	0.8%	2.7%
	Single motor	80.0%	15.8%	0.8%	3.4%

VII. Conclusion

In this paper, a electromechanical flywheel hybrid system for electric vehicle was developed. The topological structure and parameters of the hybrid system were analyzed and optimized. A vehicle dynamic simulation model was designed to study the dynamic and economic performances of the electromechanical flywheel hybrid electric vehicle under different conditions. The following conclusions were confirmed.

(1) By adopting the scheme of sun gear connecting with motor, ring gear connecting withflywheel and planet carrier connecting with output shaft, the proposed electromechanical flywheel hybrid device is able to achieve the greatest amplification of output torque, which is beneficial for the integrated and miniaturized design of the device.

(2) The maximum energy storage of the flywheel is influenced by the comprehensive factors of the volume, the mass, as well as the effective coverage of the braking energy recovery storage and the driving energy.

(3) Owing to the high power output advantage, the electromechanical flywheel hybrid device is able to improve the climbing performance and acceleration performance significantly.

(4) The front motor of the electromechanical flywheel hybrid electric vehicle adopts a miniaturized design, which can improve the working efficiency when it operates alone under the urban high-frequency and low-load conditions. Under J1015, NEDC and HWFET cycles, the average efficiency of the powertrain system increased by 8.2%, 5.6% and 4.3%, respectively.

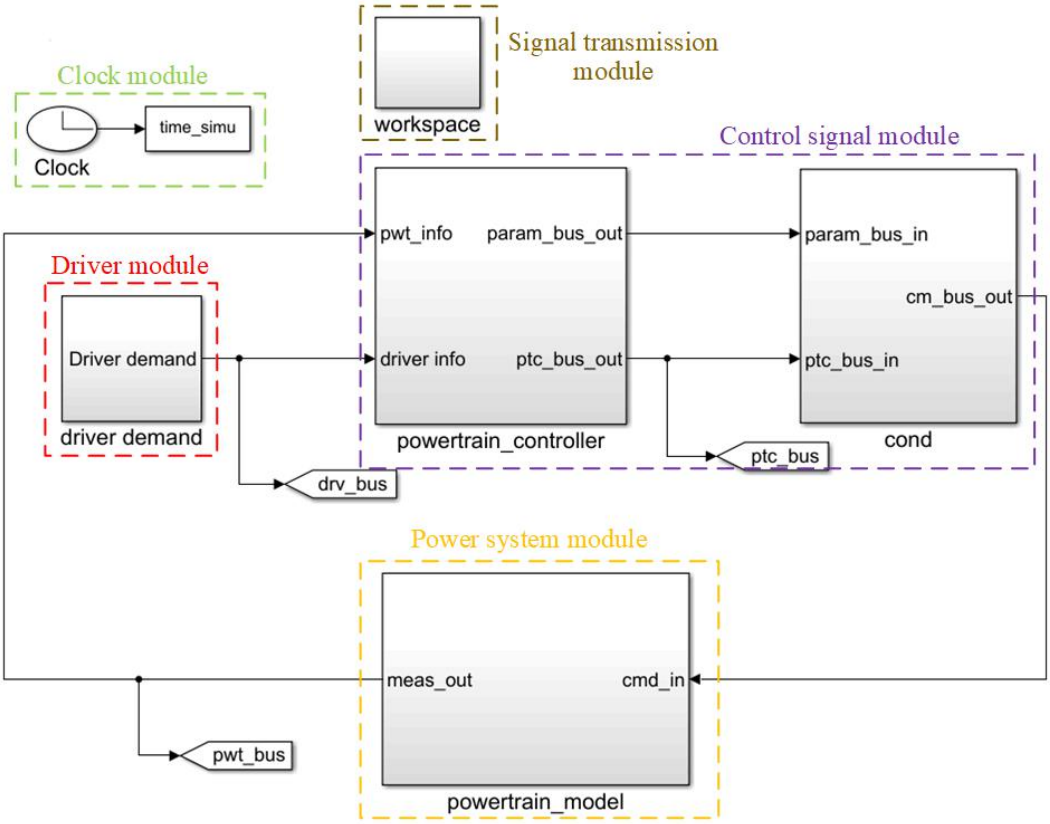

Fig. 2 The dynamics simulation platform of the electric vehicle

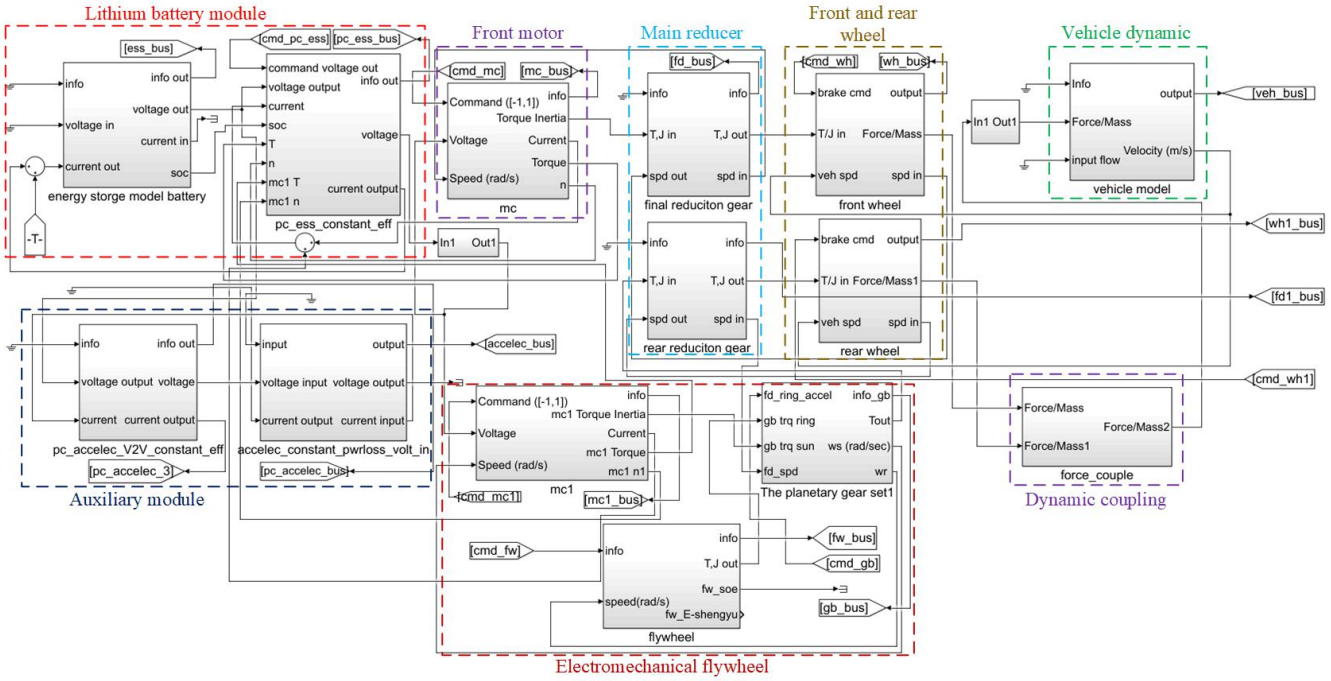

Fig. 3 Powertrain system model

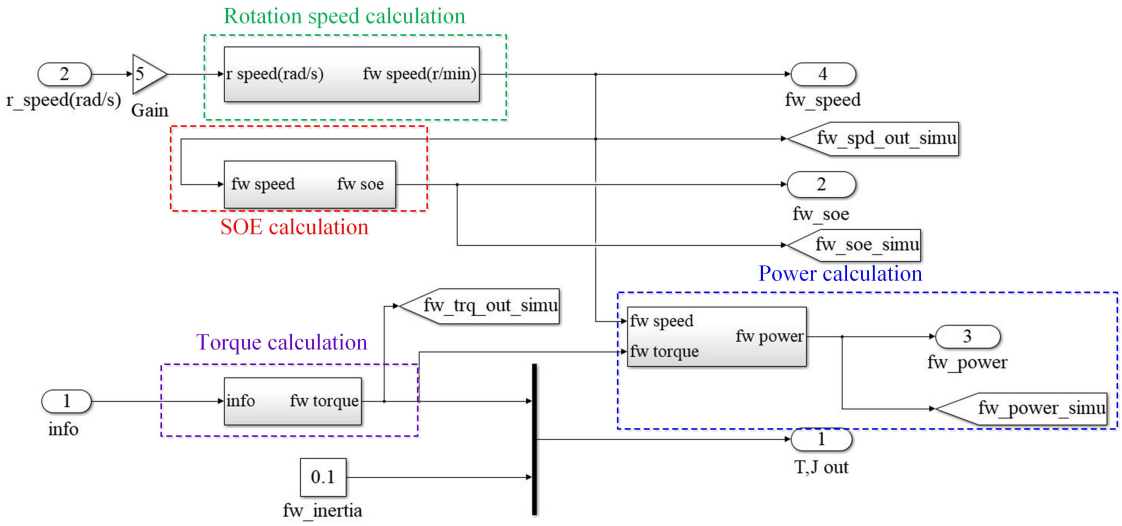

Fig. 4 Flywheel model

REFERENCES

[1] China Energy Development Strategy Research Group, "China Energy Development Strategy Selection," Beijing: Tsinghua University Press, 2013.

[2] Wen Hua Cui, Jie Sheng Wang, and Yuan Yuan Chen, "Equivalent Circuit Model of Lead-acid Battery in Energy Storage Power Station and Its State-of-Charge Estimation Based on Extended Kalman Filtering Method," Engineering Letters, vol. 26, no.4, pp504-517, 2018.

[3] Strategy advisory committee on energy-saving and new energy vehicle technology roadmap, Chinese Society of Automotive Engineering, "Energy-Saving and New Energy Vehicle Technology Roadmap," Beijing: Machinery Industry Press, 2016.

[4] Hao Tang, Yi Chun Wu, Song Song Liu, et al., "The Research of the Reuse of Degraded Lithium-ion Batteries from Electric Vehicles in Energy Storage Systems for China," Engineering Letters, vol. 29, no.4, pp1303-1310, 2021.

[5] Xin Mei Yuan, Chuan Pu Zhang, Guo Kai Hong, et al., "Method for evaluating the real-world driving energy consumptions of electric vehicles," Energy, vol. 141, pp1955-1968, 2017.

[6] Chung Neng Huang, Yui Sung Chen, "Design of magnetic flywheel control for performance improvement of fuel cells used in vehicles," Energy, vol. 118, pp840-852, 2017.

[7] A. Dhand, K. Pullen, "Review of flywheel based internal combustion engine hybrid vehicles," International Journal of Automotive Technology, vol. 14, no.5, pp797-804, 2013.

[8] A. Dhand, K. Pullen, "Review of Battery Electric Vehicle Propulsion Systems Incorporating Flywheel Energy Storge," International Journal of Automotive Technology, vol. 16, no.3, pp487-500, 2015.

[9] J. G. R. Hansen, D. U. O'Kain, "An Assessment of Flywheel High Power Energy Storage Technology for Hybrid Vehicles," Oak Ridge National Laboratory, 2012.

[10] A.A. Khodadoost Arani, H. Karami, G.B. Gharehpetian, et al., "Review of flywheel energy storage systems structures and applications in power systems and microgrids," Renewable and Sustainable Energy Reviews, vol. 69, pp9-18, 2017.

[11] B. Sun, S. Gao, C. Ma, "System Power Loss Optimization of Electric Vehicle Driven by Front and Rear Induction Motors," International Journal of Automotive Technology, vol. 19, no.1, pp121-134, 2018.

[12] Sun Binbin, Gao Song, Wu Zhe, Li Junwei, "Parameters design and economy study of an electric vehicle with powertrain systems in front and rear axle," International Journal of Engineering Transactions A: Basics, vol. 29, no.4, pp454-463, 2016.